

# Generative Model Adversarial Training for Deep Compressed Sensing

Ashkan Esmaili \*

June 22, 2021

## Abstract

Deep compressed sensing assumes the data has sparse representation in a latent space, i.e., it is intrinsically of low-dimension. The original data is assumed to be mapped from a low-dimensional space through a low-to-high-dimensional generator. In this work, we propound how to design such a low-to-high dimensional deep learning-based generator suiting for compressed sensing, while satisfying robustness to universal adversarial perturbations in the latent domain. We also justify why the noise is considered in the latent space. The work is also buttressed with theoretical analysis on the robustness of the trained generator to adversarial perturbations. Experiments on real-world datasets are provided to substantiate the efficacy of the proposed *generative model adversarial training for deep compressed sensing*.

**Index Terms** — deep compressed sensing, adversarial training, trust-region optimization, Lipschitz regularization, latent space.

## 1 Introduction and Related Work

Classical compressed sensing (CS) Candès and Wakin [2008] is built upon mapping a class of high-dimensional data into a low-dimensional one with the capability to reconstruct the high-dimensional data. Mathematically, classical CS can be formalized as

$$\mathbf{y} = \Phi \mathbf{x}, \quad (1)$$

where  $\mathbf{x} \in \mathbb{R}^n$  is the high-dimensional signal, and  $\mathbf{y} \in \mathbb{R}^m$  is the sensed (compressed) signal (of lower dimension  $m \ll n$ ).

The inverse problem of *low-to-high* dimensional reconstruction (retrieving  $\mathbf{x}$  from observations  $\mathbf{y}$ ) is not a uniquely doable task unless certain *low-complexity* assumptions govern the *data* distribution along necessary conditions on *mapping/sensing* methods Candès and Wakin [2008]. Classical CS assumes the high-dimensional data  $\mathbf{x}$  is sparse (as its low-complexity assumption), i. e.,  $\|\mathbf{x}\|_0 \ll n$  or has a sparse representation in some other domain. Moreover, if certain constraints hold for the sensing matrix (the restricted isometry property (RIP) for instance Candès et al. [2011]), unique reconstruction from low-dimensional space is guaranteed.

A vast and saturated literature on reconstruction guarantees and algorithms ( $\ell_1$  programming as the most prominent one) has been developed in the past decades Candès and Wakin [2008], Eldar and Kutyniok [2012], Esmaili et al. [2016]. Detailed review of CS literature is beyond the scope of this work the proposed work centers on deep compressed sensing (DCS) models to be elaborated hereunder.

Ever-increasing works in deep learning establish the supremacy and robustness of generative models over discriminative ones Goodfellow et al. [2016]. With this in mind, the overarching goal in DCS is to employ generative models which are expected to yield more robust and meritorious DCS models compared to the classical CS models. The shortcoming in the classical CS model is narrowing down the *information-theoretical* low-dimensional input space into a limited class of the so-called *k*-sparse signals. Nevertheless, high-dimensional data can be generated from a low-dimensional latent space, where the low-complexity structure is implicitly captured as the embedded data lie on a low-dimensional latent space. This model is expected to be more robust in introducing sparse signals derived from  $\mathbb{R}^k \rightarrow \mathbb{R}^n$  mappings, since more diversity underlies such mappings leveraging deep learning generative models compared to the classical CS *k*-sparse signals. Moreover, it is expected that more robustness to adversarial perturbations is achieved in DCS thanks to the generative model power.

\*Ashkan Esmaili is with the Electrical and Computer Engineering Department, University of Central Florida (email: ashkan.esmaili@ucf.edu).

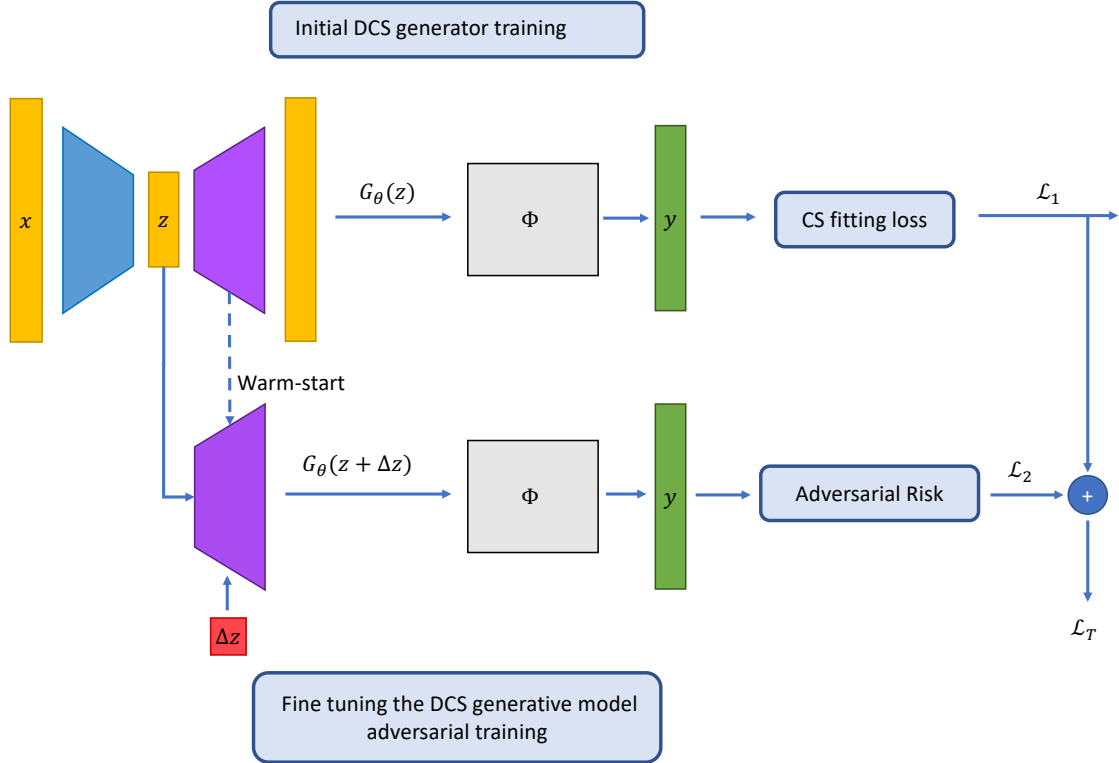


Figure 1: The schematic representation of the deep compressed sensing adversarial training procedure set forth in the paper.

After this prelude, the mathematical representation of the DCS is given as  $y = \Phi G_{\theta}(z)$ , where  $G_{\theta}$  is the deep learning based  $\mathbb{R}^k \rightarrow \mathbb{R}^n$  generator. One can find utilization of generative models in DCS and how they generalize beyond classical CS models in Wu et al. [2019], Mardani et al. [2017], Bora et al. [2017], Mardani et al. [2018], Sun et al. [2020], Van Veen et al. [2018]. There exists certain works which address the robust deep compressed sensing for defending against adversarial attack. The most important and relevant works are done by Jalal et al. [2017] and Jalal et al. [2020] in robust DCS adversarial training (DCSAT). There are three main differences which distinguish our proposed work from the line of thought in the aforementioned: **1-** The adversarial risk in our setting is considered on the sensed domain rather than the high-dimensional signal (generator's output). **2-** In our work, we consider controlling the maximal perturbation only centering on real samples (images) to be sensed rather than sweeping for maximal deviation in the generators output space which is both a highly non-convex and high dimensional problem with exhaustive search space. Additionally, it exerts harsher design constraints on the generator compared to the former scenario. **3-** In Jalal et al. [2017], the generator is pre-trained and the adversarial perturbation affects the final model through the generator output. Contrarily, in our case, we assume certain latent representations (sparse domain) are available and translate the input noise to the latent space noise. The reason we consider the noise in the latent space in our model is two-folded: 1- Many practical systems such as communication systems assume that the signal which is encoded, i.e., the input signal to the channel is directly affected by the additive noise. 2- The adversarial signal can be considered as non-robust features in the latent domain. It has been shown (as in Moosavi-Dezfooli et al. [2017], Akhtar et al. [2018]) that the perturbations in the latent space can be universal generalizable to a wide range of data.

Our method adapts and train the generator such that the robustness is realized for perturbations in the latent space. Further elaborations are provided through the paper body. Several applications rely on supremacy of DCS models including medical resonance imaging (MRI) Mardani et al. [2017], Li et al. [2019], Quan et al. [2018], Yi et al. [2019], Jiang et al. [2019], Qiusheng et al. [2020], Lee et al. [2017] and wireless neural recording Sun et al. [2016].

## 2 Deep Compressed Sensing Adversarial Training

In this section, we propose our DCSAT procedure as depicted in Fig. 1. The desired problem to train the generator equipped against adversarial attack can be cast as <sup>1</sup>,

$$\hat{\theta}(\lambda) = \underset{\theta}{\operatorname{argmin}} \left[ \mathbb{E}_{(z,y) \sim p(z,y)} \left\{ \underbrace{\max_{\|\Delta z\|_2 \leq \varepsilon} \|y - \Phi G_{\theta}(z + \Delta z)\|_2^2}_{\text{Adversarial risk}} + \lambda \underbrace{\|y - \Phi G_{\theta}(z)\|_2^2}_{\text{Fitting loss}} \right\} \right] \quad (2)$$

The overall optimization (2) is carried out over the generator parameters  $\theta$  so that two objectives (as characterized with braces) are met simultaneously, **1**- Nullifying the adversarial risk term which denotes the maximum deviation resulted from the adversarial attack  $\Delta z$  in the latent space. **2**- The second term is the CS fitting loss which aims to satisfy the DCS equation  $y = \Phi G_{\theta}(z)$ . It worth noting (as shown later) that the first term acts like a regularization on the generator parameters and prevents overfitting resulted from the second term. In addition, the coefficient  $\lambda$  establishes a trade-off between the induced regularization effect and the fitting term precision. One can consider the perturbation in the original domain which translates to some  $\Delta z$  in the latent space.

## 3 Proposed Method

In this section, we expand on the DCSAT procedure. The first order approximation for the generator  $G_{\theta}$  can be written as:

$$G_{\theta}(z + \Delta z) = G_{\theta}(z) - \mathcal{J}_G(z; \theta) \Delta z \quad (3)$$

, where  $\mathcal{J}_G(z; \theta)$  is the Jacobian matrix of the generator function w.r.t  $\theta$ . Using the first order approximation, we simplify the adversarial risk so as to make it explicitly interpretable. Next, our proposed algorithm is built upon this simplification.

Let  $\hat{y} = y - \Phi G_{\theta}(z)$  and  $\Phi \mathcal{J}_G(z; \theta)$  denote  $P$ . As observed in P (2), the adversarial risk loss value is obtained from a constrained optimization on  $\Delta z$  as the adversarial perturbation norm is limited. This leads to a quadratically constrained quadratic programming (QCQP) as follows:

$$\begin{aligned} \min_{\Delta z} \quad & -\Delta z^T P^T P \Delta z + 2\hat{y}^T P \Delta z - \|\hat{y}\|_2^2 \\ \text{subject to} \quad & \|\Delta z\|_2 \leq \varepsilon \end{aligned} \quad (4)$$

P (4) is a trust-region problem and has a solution if and only if  $\|z\| \leq \varepsilon$  and there exists  $\mu \geq 0$  such that:

$$\mathbf{1.} \quad (-P^T P + \mu I) \Delta z = -P^T \hat{y} \quad (5)$$

$$\mathbf{2.} \quad (-P^T P + \mu I) \succeq \mathbf{0} \quad (6)$$

$$\mathbf{3.} \quad \mu(\varepsilon - \|\Delta z\|_2) = 0 \quad (7)$$

It follows from (6) that  $\mu \geq \operatorname{eigmax}(P^T P)$ . Hence, (7) leads to  $\|\Delta z\|_2 = \varepsilon$ . Also, from (5) we have:

$$\Delta z = -(\mu I - P^T P)^{-1} P^T \hat{y} \quad (8)$$

Let  $P = U \Sigma V^T$  denote the singular value decomposition (SVD) for  $P$ . Using the SVD representation in Eq. 8, by expansion we obtain:  $\Delta z = -V \operatorname{diag} \left\{ \frac{\Sigma_{ii}}{\mu - \Sigma_{ii}^2} \right\} U^T \hat{y}$ , from which the norm constraint equality on  $\Delta z$  follows as:

$$\left\langle \operatorname{diag} \left\{ \frac{\Sigma_{ii}}{\mu - \Lambda_{ii}} \right\}, U^T \hat{y} \right\rangle^2 = \hat{y}^T U \operatorname{diag} \left\{ \frac{\Lambda_{ii}}{(\mu - \Lambda_{ii})^2} \right\} U^T \hat{y} = \varepsilon^2 \quad (9)$$

<sup>1</sup>Each signal in the original domain  $x$ , is characterized by a representation in the latent domain  $z$  as  $x = G_{\theta}(z)$ . Hence, the joint distribution  $p(x,y) = f_{\theta}(p(z,y))$  can be expressed through a 1-1 mapping relating it to the joint distribution between sensed signals and the latent representation samples.

### 3.1 Explicit Upper Bound for Adversarial Risk

Utilizing the Cauchy-Schwartz inequality, the matrix operator norm inequality, and the energy constraint for  $\Delta z$ , the adversarial risk can be upper bounded as:

$$\Delta z^T P^T P \Delta z - 2\hat{y}^T P \Delta z + \|\hat{y}\|_2^2 \leq \|\hat{y}\|_2^2 + 2\|\hat{y}\| \|P\|_{op} \|\epsilon\| + \|P\|_{op}^2 \|\epsilon\|_2^2 \quad (10)$$

Using the fact that  $|ab| \leq \frac{a^2+b^2}{2}$ , the latter can be upper bounded with  $2\|\hat{y}\|_2^2 + 2\|P\|_{op}^2 \epsilon^2$ . The upper bound is used in order to be make the adversarial risk explicitly expressible in terms of the network parameters and as a result, derive simpler algorithm for evaluating back-propagation gradient flows in training the generator. Although this is an upper bound, we establish in the following section that it is not a loose upper bound, i. e., minimizer of the upper bound also pushes down the proposed adversarial risk in P (2). Substituting the upper bound instead of the original adversarial risk, the dependency of the optimization problem on  $\Delta z$  is dropped, and the resulted function is explicitly parameterized only on the generator parameters  $\theta$  as:<sup>2</sup>

$$\hat{\theta}(\lambda) = \underset{\theta}{\operatorname{argmin}} \left\{ \mathbb{E}_{(z,y) \sim p(z,y)} \left\{ \|\Phi \mathcal{J}_G(z; \theta)\|_{op}^2 \epsilon^2 + \frac{\lambda+1}{2} \|y - \Phi G_\theta(z)\|_2^2 \right\} \right\} \quad (12)$$

In training with back propagation, obtaining the gradient flow for the fitting loss is straightforward and can be evaluated as  $\mathcal{J}_G^T(\theta) \Phi^T (y_i - \Phi G_\theta(z_i))$ . Yet, the approximation of the adversarial risk which contains the Jacobian  $\mathcal{J}_G(z; \theta)$  must be explicitly expressed based on the network parameters which is considered in the following lemma Zhang et al. [2019].

**Lemma 1.** *Assume the generator  $G_\theta$  is an  $H$ -layer neural network. The Jacobian  $\mathcal{J}_G(\theta)$  can be written as:*

$$W^H D^H \dots W^1 D^1, \quad (13)$$

where  $D^i$ 's are diagonal matrices containing the derivatives of the activation functions and  $W^i$ 's are the dense layer matrices.

In order to minimize the operator norm of the product  $P = \Phi \mathcal{J}_G(G_\theta; z)$ , one can bound the operator norms of the layers  $W^l$  which constitute the Jacobian as specified in lemma 3.1. Owing to the Cauchy-Schwartz inequality for the product of matrices, the overall operator norm will be also bounded and regularized. We implement this by exerting the loss  $\|\mathbf{I} - W^T W\|_F^2$ , whose gradient is explicitly derivable, in place of the Jacobian operator norm term in P (12). Such regularization perform Lipschitz projection of the  $W$  layers. In DCS setting, the sensing matrix can be considered as the final dense layer. However, it is constant and not trainable. Accordingly, Lipschitz regularization cannot be applied on  $\Phi$ . Instead, we project as much energy of  $W^H$  (the last layer) to the null-space of the sensing matrix  $\Phi$  by regularizing  $\|\Phi W\|_{op}$ . It is worth noting that although such regularizations help mitigating the adversarial attack effect, they also limit the learning and exploration capability of the model. A compromise between the CS fitting loss and the adversarial risk through tuning  $\lambda$  determines the extent to which the regularizations are employed (The ensemble parameters  $W^l, D$  are denoted in  $\theta$ ).

### 3.2 Why Do Upper Bound Optimal Parameters Also Apply to the Original Adversarial Risk?

Substituting the closed form  $\Delta z$  in objective function (4), we have:

$$\mathcal{L} = \hat{y}^T U \operatorname{diag} \left\{ 1 + \frac{2\Lambda_{ii}}{\mu - \Lambda_{ii}} + \frac{\Lambda_{ii}^2}{(\mu - \Lambda_{ii})^2} \right\} U^T \hat{y}. \quad (14)$$

Now, we adjudicate how minimizing the approximated upper bound instead of the proposed adversarial risk, and using the achieved parameters also decreases the adversarial risk function in P (2). If the operator norms of  $W^l$ 's are regularized, the exploration of the learning function reduces which ends up with higher fitting loss  $\hat{y}$ . The benefit of regularization towards mitigating the adversarial risk during the training procedure must outweigh the model learning degradation (i. e., increase in the fitting loss  $\hat{y}$ ) to yield an acceptable adversarial training. If the coefficient  $\lambda$  is set to a large value in P (2), only slight increase in  $\hat{y}$  is tolerable as a result of regularization. Otherwise, the large coefficient

<sup>2</sup>Working with training samples, the expectation in optimization (12) is substituted with summation over training samples, i. e., pairs of  $(z_i, y_i)$ .

$$\hat{\theta}(\lambda) = \underset{\theta}{\operatorname{argmin}} \sum_{i=1}^n \left\{ \|\Phi \mathcal{J}_G(z_i; \theta)\|_{op}^2 \epsilon^2 + \frac{\lambda+1}{2} \|y_i - \Phi G_\theta(z_i)\|_2^2 \right\} \quad (11)$$

$\lambda$  leads to a large gap  $\lambda\Delta\hat{y}$  that can not be compensated through the positive effect of regularization applied through adversarial risk. Thus, the change in  $\hat{y}$  becomes negligible with a large choice for  $\lambda$  (regularization coefficient for fine-tuning  $G_\theta$ ). Also, the basis span in SVD for  $\mathcal{J}_G(\theta)$  and as a result in  $P$  is assumed not to rotate as the proposed Lipschitz projection simply regularizes the singular values and does not change the exploring subspace found for  $W$  layers meaning that  $U$  and therefore  $U^T\hat{y}$  are invariant. With this in mind, taking a look back into the norm constraint Eq. (9),  $\Lambda_{ii}$ s are reduced after regularization. Unless  $\mu$  is reduced appropriately, the equality would not be maintained. Now, consider the loss in Eq. (14). The change in the first term was forced to be negligible by proper choice for  $\lambda$ . We write the second and third diagonal terms as  $2\frac{\Sigma_{ii}}{(\mu-\Lambda_{ii})}\Sigma_{ii}$  and  $\frac{\Lambda_{ii}}{(\mu-\Lambda_{ii})^2}\Lambda_{ii}$ , respectively. In both fractions, the first term is invariant, and the second terms are eigenvalues which are regularized (reduced). Hence, the whole term shrinks leading to shrinkage of the original adversarial risk. All in all, addressing Lipschitz property for the surrogate optimization leads to smaller adversarial risk in the main proposed optimization and the upper bound surrogate is not a loose upper bound whose minimizer leaves no change in the original adversarial risk. Heuristically,  $\mu$  decreases proportional to  $\Lambda_{ii}$ . Hence, the  $\mu^2$  appearing in the nominator of the original adversarial risk decreases quadratically reducing the loss function more.

## 4 Numerical Experiments

Images and in general large data arrays may be sensed only partially (a.k.a) missing data due to limitations in imaging devices (include example for MRI) or corrupt measurements.

In this work, we assume the sensing matrix is a random sampler which partially masks the images. This resembles the missing data and inference using a model-based structure on data. Rather than classical low-rank assumptions (as in Azghani et al. [2019], Esmaeili et al. [2018], Esmaeili and Marvasti [2019]) we use the intrinsic low-dimensionality of latent space mapped with a deep learning model.

The objective is to reconstruct the original samples from the randomly sampled image. With such sensing method, which happens to be common in many practical applications, the attacker can invest only on parts of signal which happen to have overlap with the sensing matrix mask and hence, effectively expend the perturbation energy on the mask. Hence, a sampling mask makes the defensive training of the generator more difficult.

### 4.1 Applying Adversarial Attack

Next, we investigate the efficacy of our generative model DCSAT method in mitigating adversarial attack for certain simulation scenarios. In order to apply the adversarial attack, we use omni-directional  $\Delta\mathbf{z}$  directions around the initial latent sample and make consecutive queries to pick the maximum deviation in the sensed generator’s output as the adversarial attack. This is an empirical approach to find the adversarial attack.

### 4.2 MNIST Dataset

In this experiment, we have considered a generator consisting of two consecutive dense layers, mapping from the latent space with size 30 to 100, and from 100 to 784 (output image size). Next, the output is sensed with a random sampling matrix. The latent space representation of the MNIST data is obtained through a compressing decoder which maps data through two dense layers from 784 to 100 and 100 to 30, respectively. The encoder and decoder can be trained using an auto-encoder. After training the auto-encoder, the generator part is removed from the auto-encoder in order to be fine-tuned for DCS adversarial training. It can benefit from the warm-start obtained from training the auto-encoder. The latent representations are also stored to be utilized further as the generator input for generating high dimensional samples. In the final step, the warm-start generator ought to be fine-tuned to both hold in the CS fitting loss as well as maintaining the discussed Lipschitz property through explicit adversarial regularizations. In the final step, we attach the sensing matrix to the last dense layer of the generator and set its trainable option to false. We train the resulted generator to map the obtained latent representations to the sensed MNIST images.

### 4.3 CIFAR-10 Dataset

In this experiment, the encoder and the decoders consist of convolutional layers rather than simple dense layers to extract local features Balntas et al. [2016]. The inputs are CIFAR-10 images of size  $(32 \times 32 \times 3)$ . The encoder consists of three Conv2D layers which are followed by batch normalization layers, relu activation layers, and (2, 2) MaxPooling2D layers. The Conv2D layers have 64, 32, and 16 filters, respectively. The kernel size is considered as (3, 3), and the stride is set to (1, 1). The decoder builds up reversely utilizing UpSampling2D to compensate for the MaxPooling2D layers. Similar to the mnist setting, an auto-encoder is trained to find the encoded latent representations. Next,

Method	$\lambda/SR$	Adv. risk	Fit. loss	total loss
DCS	—/ 0.8	5.5948	<b>4.0290</b>	9.6238
DCSAT	200,000 / 0.8	5.5114	4.0370	9.5484
DCSAT	20,000 / 0.8	5.3726	4.1051	<b>9.4777</b>
DCSAT	2,000 / 0.8	<b>5.2547</b>	4.4278	9.6825
DCS	—/ 0.6	6.2214	5.2129	11.4343
DCSAT	200,000 / 0.6	6.1611	<b>5.1508</b>	11.3119
DCSAT	20,000 / 0.6	6.0561	5.2535	<b>11.3096</b>
DCSAT	2,000 / 0.6	<b>5.8972</b>	5.4452	11.3424

Table 1: DCSAT ablation study on the MNIST test dataset.

Method	$\lambda/SR$	Adv. risk	Fit. loss	total loss
DCS	—/ 0.8	0.1375	<b>0.0184</b>	0.1559
DCSAT	10,000 / 0.8	<b>0.0839</b>	0.0192	<b>0.1029</b>
DCSAT	1000 / 0.8	0.1292	0.0213	0.1505
DCSAT	100 / 0.8	fail	0.0227	—
DCS	—/ 0.6	0.1327	<b>0.0166</b>	0.1493
DCSAT	10,000 / 0.6	<b>0.0793</b>	0.0176	<b>0.0969</b>
DCSAT	1000 / 0.6	0.1202	0.0194	0.1396
DCSAT	100 / 0.6	fail	0.0235	—

Table 2: DCSAT ablation study on the CIFAR-10 test dataset. Larger errors for MNIST are due to early stopping (fewer epochs for fine-tuning).

the decoder part can be fine-tuned via the proposed DCSAT to robustify the generator against adversarial perturbations while maintaining desired DCS precision.

#### 4.4 Simulation Result Analysis

In this section, we discuss the simulation results and provide examples of how adversarially training the generator. In this section, we discuss the simulation results on test sets. Tables 1 and 2 include an ablation study of two hyper parameters: 1- the adversarial/fitting loss trade-off ( $\lambda$ ), and 2- two sampling rates (SR) (80% and 60%) for the sensing matrix  $\Phi$ . The regularization parameter  $\lambda$  compromises between the model robustness to perturbations and the learning capacity. More regularization induce learning bottleneck for the model. However, as observed, regularization conversely affects fitting loss and best fitting loss values are related to DCS implementation where there is no adversarial training (except for one instance due to the overfitting effect). Contrarily, increasing  $\lambda$ , the adversarial risk goes down except for ( $\lambda < 1000$ ) in CIFAR-10 experiment where the regularization bottleneck makes the model malfunction in learning. The optimal values are highlighted in bold. It is worth mentioning that the optimal design (minimal aggregate loss) is obtained from a hyper-parameter tuned DCSAT scenario and not the sole DCS which clarifies the supremacy of DCSAT over DCS. Fig.2 shows the splitting behavior in training DCSAT and DCS models.<sup>3</sup>

## 5 Conclusion

Deep compressed sensing is a more robust framework compared to classical CS. Adversarial attackers try to lower a system performance by triggering the signals in low-dimensional latent space resulting in significant variation of the sensed output. In this work, we have shown how to train a deep compressed sensing generator which is robust to the effect of universal perturbations triggered in the latent space as well as mapping data to the compressed sensing domain to suit for the compressed sensing loss. The work is buttressed with math analysis on how the applied method helps reduce the adversarial effect. Real-world compressed sensing experiments verify the efficacy of the proposed procedure in training the deep compressed sensing generator.

<sup>3</sup>The experiments are available at <https://github.com/ashkanucf/DCSAT.git>.

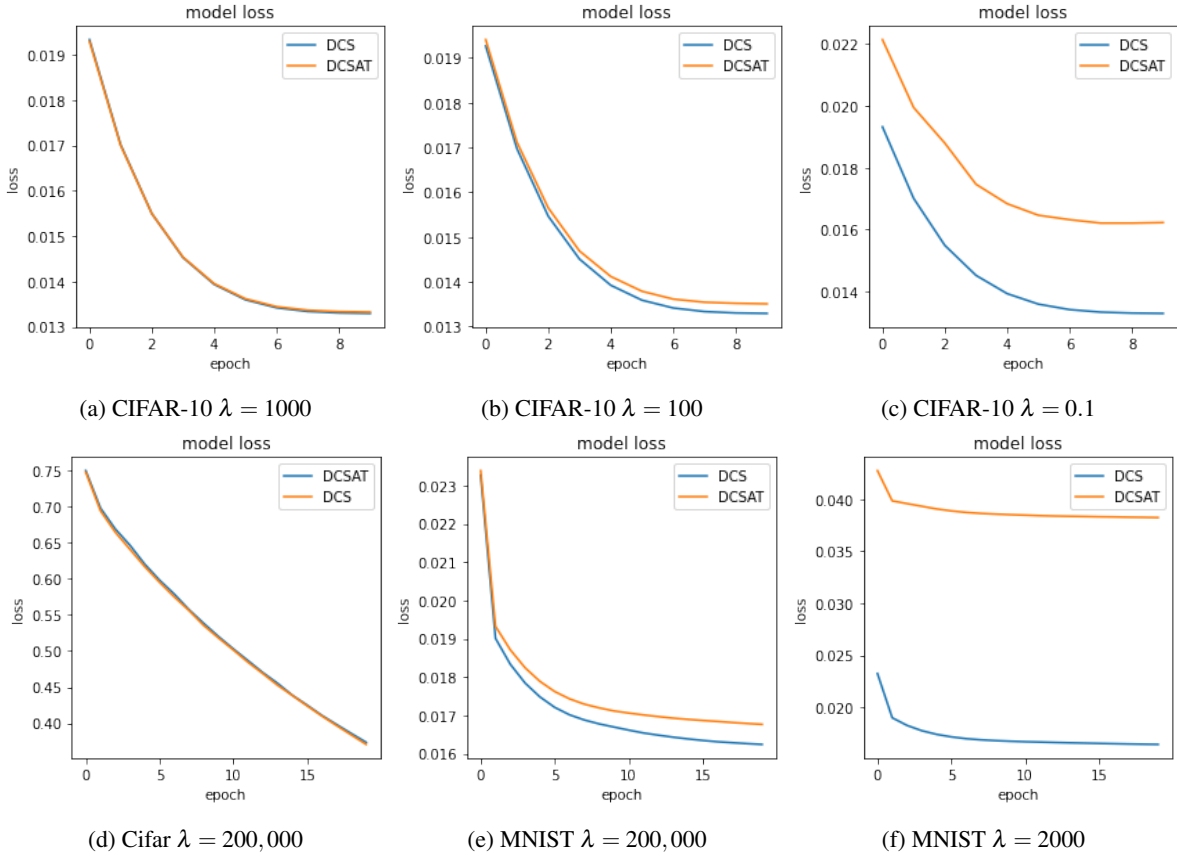


Figure 2: Comparison of DCS vs. DCSAT training error for different regularization levels ( $SR = 80\%$ ).

## References

- Naveed Akhtar, Jian Liu, and Ajmal Mian. Defense against universal adversarial perturbations. In *Proceedings of the IEEE Conference on Computer Vision and Pattern Recognition*, pages 3389–3398, 2018.
- Masoumeh Azghani, Ashkan Esmaeili, Kayhan Behdin, and Farokh Marvasti. Missing low-rank and sparse decomposition based on smoothed nuclear norm. *IEEE Transactions on Circuits and Systems for Video Technology*, 30(6): 1550–1558, 2019.
- Vassileios Balntas, Edgar Riba, Daniel Ponsa, and Krystian Mikolajczyk. Learning local feature descriptors with triplets and shallow convolutional neural networks. In *Bmvc*, volume 1(2), page 3, 2016.
- Ashish Bora, Ajil Jalal, Eric Price, and Alexandros G Dimakis. Compressed sensing using generative models. *arXiv preprint arXiv:1703.03208*, 2017.
- Emmanuel J Candès and Michael B Wakin. An introduction to compressive sampling. *IEEE signal processing magazine*, 25(2):21–30, 2008.
- Emmanuel J Candes, Yonina C Eldar, Deanna Needell, and Paige Randall. Compressed sensing with coherent and redundant dictionaries. *Applied and Computational Harmonic Analysis*, 31(1):59–73, 2011.
- Yonina C Eldar and Gitta Kutyniok. *Compressed sensing: theory and applications*. Cambridge university press, 2012.
- Ashkan Esmaeili and Farokh Marvasti. A novel approach to quantized matrix completion using huber loss measure. *IEEE Signal Processing Letters*, 26(2):337–341, 2019.
- Ashkan Esmaeili, Ehsan Asadi, and Farokh Marvasti. Iterative null-space projection method with adaptive thresholding in sparse signal recovery and matrix completion. *arXiv preprint arXiv:1610.00287*, 2016.

- Ashkan Esmaeili, Kayhan Behdin, Mohammad Amin Fakharian, and Farokh Marvasti. Transduction with matrix completion using smoothed rank function. *arXiv preprint arXiv:1805.07561*, 2018.
- Ian Goodfellow, Yoshua Bengio, Aaron Courville, and Yoshua Bengio. *Deep learning*, volume 1. MIT press Cambridge, 2016.
- Ajil Jalal, Andrew Ilyas, Constantinos Daskalakis, and Alexandros G Dimakis. The robust manifold defense: Adversarial training using generative models. *arXiv preprint arXiv:1712.09196*, 2017.
- Ajil Jalal, Liu Liu, Alexandros G Dimakis, and Constantine Caramanis. Robust compressed sensing of generative models. *arXiv preprint arXiv:2006.09461*, 2020.
- Mingfeng Jiang, Zihan Yuan, Xu Yang, Jucheng Zhang, Yinglan Gong, Ling Xia, and Tieqiang Li. Accelerating cs-mri reconstruction with fine-tuning wasserstein generative adversarial network. *IEEE Access*, 7:152347–152357, 2019.
- Dongwook Lee, Jaejun Yoo, and Jong Chul Ye. Deep residual learning for compressed sensing mri. In *2017 IEEE 14th International Symposium on Biomedical Imaging (ISBI 2017)*, pages 15–18. IEEE, 2017.
- Zhongnian Li, Tao Zhang, Peng Wan, and Daoqiang Zhang. Segan: structure-enhanced generative adversarial network for compressed sensing mri reconstruction. In *Proceedings of the AAAI Conference on Artificial Intelligence*, volume 33, pages 1012–1019, 2019.
- Morteza Mardani, Enhao Gong, Joseph Y Cheng, Shreyas Vasanaawala, Greg Zaharchuk, Marcus Alley, Neil Thakur, Song Han, William Dally, John M Pauly, et al. Deep generative adversarial networks for compressed sensing auto-mates mri. *arXiv preprint arXiv:1706.00051*, 2017.
- Morteza Mardani, Enhao Gong, Joseph Y Cheng, Shreyas S Vasanaawala, Greg Zaharchuk, Lei Xing, and John M Pauly. Deep generative adversarial neural networks for compressive sensing mri. *IEEE transactions on medical imaging*, 38(1):167–179, 2018.
- Seyed-Mohsen Moosavi-Dezfooli, Alhussein Fawzi, Omar Fawzi, and Pascal Frossard. Universal adversarial perturbations. In *Proceedings of the IEEE conference on computer vision and pattern recognition*, pages 1765–1773, 2017.
- Lian Qiusheng, Fan Xiaoyu, Shi Baoshun, and Zhang Xiaohua. Compressed sensing mri based on the hybrid regularization by denoising and the epigraph projection. *Signal Processing*, 170:107444, 2020.
- Tran Minh Quan, Thanh Nguyen-Duc, and Won-Ki Jeong. Compressed sensing mri reconstruction using a generative adversarial network with a cyclic loss. *IEEE transactions on medical imaging*, 37(6):1488–1497, 2018.
- Biao Sun, Hui Feng, Kefan Chen, and Xinshan Zhu. A deep learning framework of quantized compressed sensing for wireless neural recording. *IEEE Access*, 4:5169–5178, 2016.
- Yubao Sun, Jiwei Chen, Qingshan Liu, and Guangcan Liu. Learning image compressed sensing with sub-pixel convolutional generative adversarial network. *Pattern Recognition*, 98:107051, 2020.
- Dave Van Veen, Ajil Jalal, Mahdi Soltanolkotabi, Eric Price, Sriram Vishwanath, and Alexandros G Dimakis. Compressed sensing with deep image prior and learned regularization. *arXiv preprint arXiv:1806.06438*, 2018.
- Yan Wu, Mihaela Rosca, and Timothy Lillicrap. Deep compressed sensing. *arXiv preprint arXiv:1905.06723*, 2019.
- Xin Yi, Ekta Walia, and Paul Babyn. Generative adversarial network in medical imaging: A review. *Medical image analysis*, 58:101552, 2019.
- Huan Zhang, Pengchuan Zhang, and Cho-Jui Hsieh. Recurjac: An efficient recursive algorithm for bounding jacobian matrix of neural networks and its applications. In *Proceedings of the AAAI Conference on Artificial Intelligence*, volume 33, pages 5757–5764, 2019.